Spin-Polarized Two-Dimensional Electron Gas at Oxide Interfaces

B. R. K. Nanda and S. Satpathy

Department of Physics and Astronomy, University of Missouri, Columbia, Missouri 65211, USA

(Received 19 April 2008; published 18 September 2008)

The possibility of formation of a fully spin-polarized 2D electron gas at the $SrMnO_3/(LaMnO_3)_1/SrMnO_3$ heterostructure is predicted from density-functional calculations. The La(d) electrons become confined in the direction normal to the interface in the electrostatic potential well of the positively charged layer of La atoms, acting as electron donors. These electrons mediate a ferromagnetic alignment of the Mn t_{2g} spins near the interface via Zener double exchange and become, in turn, spin-polarized due to the internal magnetic fields of the Mn moments.

DOI: 10.1103/PhysRevLett.101.127201 PACS numbers: 75.70.Cn, 71.10.Ca, 71.20.−b, 73.20.−r

Recent advances in the fabrication of high-quality epitaxial interfaces between perovskite oxides have led to a rapid surge of interest in the study of new interface electronic states. A number of oxide interfaces have been shown to possess electrons confined to the interface region forming a two-dimensional electron gas (2DEG). A clear example is an isolated [100] monolayer of $LaTiO_3$ grown in a $SrTiO_3$ host [1–4]. The trivalent La substituting for the divalent Sr in essence behaves as a positively charged layer of electron-donor dopants producing a wedge-shaped potential at the interface, where the electrons become confined. A similar type of electron gas has been observed at the much-studied $LaAlO_3/SrTiO_3$ interface [5], although the exact origin of the electron gas there remains controversial. A somewhat different physics resulting from the interface polarization charges produces the 2DEG at the nitride and the oxide interfaces such as $GaN/Al_xGa_{1-x}N$ [6] and $ZnO/Mg_xZn_{1-x}O$ [7]. These electron gases often show clear Shubnikov–de Haas oscillations, and even superconductivity has been observed in one of the systems [8].

Since many of these oxides contain magnetic atoms as well, the question arises as to whether one may be able to get a spin-polarized electron gas at the interface, using the internal magnetic fields of the magnetic atoms. In this Letter, we predict from calculations based on the density-functional theory (DFT) the existence of just such a phase at the manganite heterostructure consisting of a $LaMnO_3$ (LMO) monolayer embedded in the $SrMnO_3$ (SMO) bulk, sketched in Fig. 1.

The results presented here are obtained from the DFT studies of the $(LMO)_1/(SMO)_7$ layered superlattice using the linear augmented plane wave (LAPW) [9] and the linear muffin-tin orbitals (LMTO) methods [10] with the generalized gradient approximation (GGA) [11] or the Coulomb-corrected local spin density approximation (LSDA + U). The supercell consisted of twice this formula unit because of the magnetic structures considered in the Letter. The structural relaxation was performed using the LAPW-GGA method for the magnetic structure. The calculated cubic lattice constant for the La compound is 3.915 Å and for the Sr compound is 3.802 Å, which are close to the experimental values of 3.935 and 3.805 Å, respectively. For the relaxed structure, we fixed the in-plane lattice parameter of the superlattice to be 3.802 Å corresponding to the bulk lattice constant of the Sr compound. This was also the lattice constant for the SMO part in the direction normal to the superlattice, while the same for the LMO monolayer was taken to be 4.15 Å, which preserves the volume of the LMO unit cell in the bulk. The atomic positions were then relaxed along the c axis.

The results, presented in Fig. 2, indicate the movement of the cations away from the interface, while the anions move towards the interface due to the electrostatic attraction of the La layer. This is similar to the cation-anion polarization obtained for the $(SrTiO_3)_n/(LaTiO_3)_1$ heterostructure, where there also exists at the interface a positively charged La layer [3,4,12]. The electronic structure for the relaxed lattice was obtained using the LMTO method with the LSDA + U approximation, using the Coulomb and exchange parameters of $U = 5$ eV and $J = 1$ eV, respectively.

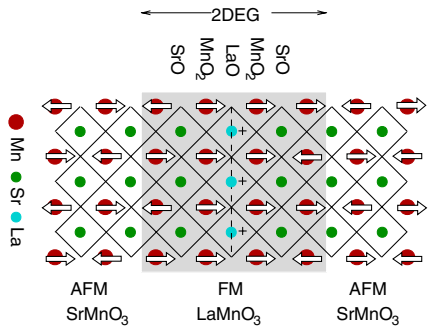

FIG. 1 (color online). The manganite heterostructure with a monolayer of $LaMnO_3$ embedded in the $SrMnO_3$ bulk, with the shadowed region indicating the spin-polarized 2DEG confined to the interface region. Oxygen atoms occur at the intersections of the checkered lines forming the MnO_6 octahedra.

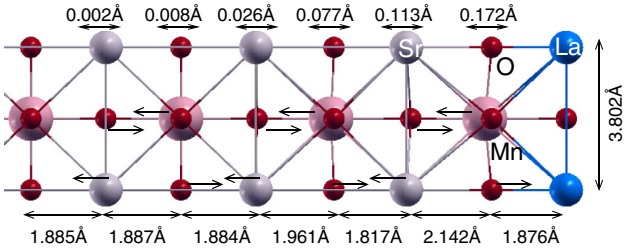

FIG. 2 (color online). Relaxed atomic positions for the $(LMO)_1/(SMO)_7$ superlattice with arrows showing the atomic displacements. The bottom numbers indicate the positions of the O planes, while the numbers on top indicate the cation-anion polarizations (positions of Mn/Sr with respect to the O planes), which diminish quickly away from the interface.

The magnetic ground states of the two bulk compounds are very different. While SMO with its Mn^{4+} $(t_{2g}^3 e_g^0)$ configuration is a G-type antiferromagnet (AFM) with the magnetic interaction between the Mn core spins driven by superexchange [13], LMO is an A-type antiferromagnet with a Mn^{3+} $(t_{2g}^3 e_g^1)$ electronic configuration, with the partially filled e_g electrons mediating a ferromagnetic double exchange between the t_{2g} core spins on the MnO_2 planes [14,15]. For the present interface, there is just one extra electron per La atom, which is localized near the interface, occupying the Mn e_g orbitals (see Fig. 3). These electrons serving as the itinerant electrons in the standard double-exchange picture [16] modify the magnetism of the Mn t_{2g} core spins.

In order to study the ground state, we have computed the total energies for several magnetic configurations. We find the lowest-energy structure to be the one shown in Fig. 1, where the two MnO_2 layers on either side of the La layer are ferromagnetic, while the remaining Mn atoms retain the Néel G-type AFM of the SMO bulk. The remaining

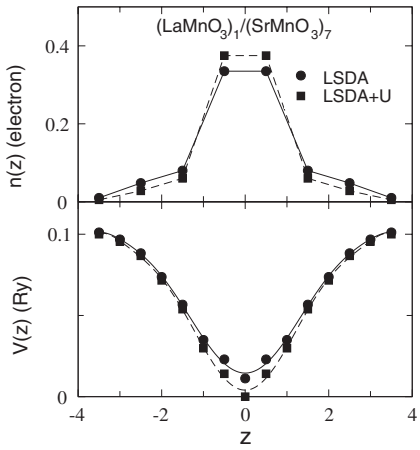

FIG. 3. The cell-averaged potential $V(z)$ calculated from Eq. (1) with distance z from the La layer in units of $SrMnO_3$ monolayer thickness (bottom) and the layer occupancy $n(z)$ of the donated electrons, one per La atom, occupying predominantly the Mn (e_g) orbitals (top).

three structures that we examined all have higher energies, viz., (i) the structure with a complete G-type magnetism, (ii) the structure where the layer ferromagnetism is extended up to the second MnO_2 layer on either side of the interface, and (iii) the structure similar to the one in Fig. 1, except that the two MnO_2 layers across the interface are aligned antiferromagnetically. The ferromagnetism at the interface is explained by the fact that the itinerant e_g electrons mediating the Zener double exchange reside mainly in the two layers at the interface, even though a small e_g charge spreads to layers beyond the first layer.

We note that the magnetic structure of the interface is very much dependent on the strain condition [17,18], so that the spin-polarized 2DEG may not exist for different strain conditions than the one studied here, where the in-plane lattice constant corresponds to the SMO bulk.

The potential seen by the electron at the interface may be calculated from the variation of the cell-averaged point-charge Coulomb potential V, which was calculated by first averaging the potential over the volume of the ith Wigner-Seitz atomic sphere [2,19]:

$$V_i = \frac{3q_i}{2s_i} + \sum_j \frac{q_j}{|r_i - r_j|} \qquad (1)$$

and then by averaging over all spheres with a weight factor proportional to their volumes Ω_i: $V = \sum_i \Omega_i V_i / \sum_i \Omega_i$, where s_i is the sphere radius, r_i its position, and q_i is the total charge, nuclear plus electronic. In Eq. (1), the first term is the sphere average of the potential of the point charge located at the center of the muffin-tin sphere, and the second term is the Madelung potential due to all other spheres in the solid. The results plotted in Fig. 3 show the screening of the bare linear potential due to the electrostatic field of the charged La plane caused by the electronic as well as the lattice polarization. The screened potential is deep enough to localize the donor electron within just a few layers of the interface. In fact, we find that about $0.7e^-$ is located on the first MnO_2 layers and $0.14e^-$ on the second layers, and the remaining $0.16e^-$ is spread between the remaining atoms.

The presence of a substantial amount of the e_g charge on the first MnO_2 layer is consistent with the double-exchange mechanism for the layer ferromagnetism (Fig. 1) found from the DFT calculations. However, although in the DFT results, the structure, where the second MnO_2 layer is also ferromagnetic in addition to the first, was not energetically favorable, the leaked e_g electrons into the second layer could result in a canted ferromagnetic state for this layer, depending on the amount of charge leakage and the strength of the double exchange.

To address this issue, we have studied the Zener-Anderson-Hasegawa double-exchange model [16] on a four-layer lattice (Fig. 4, inset), each layer being a square lattice, as appropriate for the MnO_2 layers. The model Hamiltonian, restricted to the Mn sites up to second MnO_2 planes away from the interface, is given by

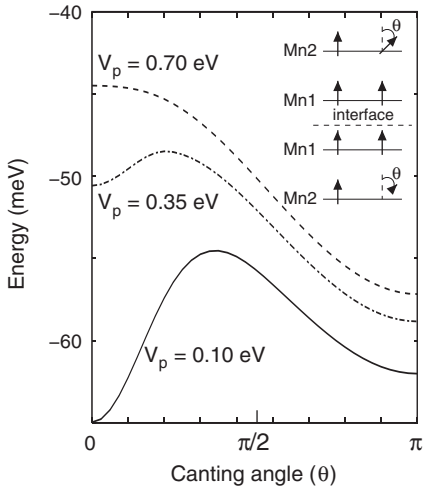

FIG. 4. Total energy obtained from Eq. (2) as a function of the canting angle between the nearest neighbor Mn spins in the second MnO_2 layer for different values of the potential V_p.

$$H = \sum_{i\sigma} \epsilon_{i\sigma} n_{i\sigma} + t \sum_{\langle ij\rangle\sigma} c^{\dagger}_{i\sigma} c_{j\sigma} + \text{H.c.} + J \sum_{\langle ij\rangle} \hat{S}_i \cdot \hat{S}_j - 2J_H \sum_i \vec{S}_i \cdot \vec{s}_i, \quad (2)$$

and it describes the double-exchange interaction of the itinerant electrons in a lattice of localized spins. Here $c^{\dagger}_{i\sigma}$ and $c_{i\sigma}$ are the field operators for the e_g carriers, treated within a one-band model, with i and σ being the site and spin indices, respectively, $\vec{S}_i$ is the localized t_{2g} spin, and $\vec{s}_i$ is the spin density of the itinerant electrons. The on-site energy $\epsilon_{i\sigma}$ (V_p on the second layer and zero on the first) describes the electric field at the interface and is the parameter that controls the leakage of the itinerant electron into the second layer. J is the superexchange between the localized spins, while J_H is the Hund's coupling between the itinerant and the localized electrons. From the earlier DFT studies of the bulk manganites [14,20,21], typical values of the parameters are $t \sim -0.15$ eV, $J \sim 7$ meV, and $J_H \sim 1$ eV. Note that, unlike our earlier work [22], here we neglect the on-site Coulomb energy between the itinerant carriers, since their number is small.

The Hamiltonian (2) is solved by diagonalizing a 16×16 Hamiltonian matrix (eight Mn atoms per unit cell and two spin types) for a number of $\vec{k}$ points in the two-dimensional Brillouin zone, and the total energy is calculated by summing over the occupied states (two electrons per cell). The results summarized in Fig. 4 show that an antiferromagnetic second layer (canting angle $\theta = \pi$) is overwhelmingly favored over a canted state for a parameter of $V_p \approx 0.5$ eV, which yields roughly the same amount of electron leakage into the second MnO_2 layer as obtained from the DFT calculations. This indicates the absence of a canted state.

The electronic structure corresponding to the lowest-energy magnetic structure (Fig. 1) is shown in Fig. 5. The t_{2g} states of one spin are occupied for each Mn atom and lie far below the Fermi energy E_F because of the octahedral crystal field produced by the MnO_6 octahedron and the strong Coulomb repulsion U. The vicinity of E_F is occupied by the Mn-e_g states. In the spin-majority channel, we see extended e_g states crossing the Fermi level, while in the spin-minority channel, they are unoccupied and open up a gap at the Fermi energy, so that we have the equivalent of a half-metallic system in two dimensions.

While there are a number of half-metallic systems known in 3D, the classic one being Fe_3O_4 [23], the present case is quite unique in the sense that the electrons at the Fermi energy are confined to the interface region, producing a fully spin-polarized 2DEG. This is in fact a key point of this Letter.

The bands crossing the Fermi energy are the majority-spin Mn1-e_g ($x^2 - y^2$ and $3z^2 - 1$) states belonging to the first-layer manganese atoms with bonding interaction across the interface. The corresponding antibonding states as well as all minority-spin Mn1-e_g states occur higher in

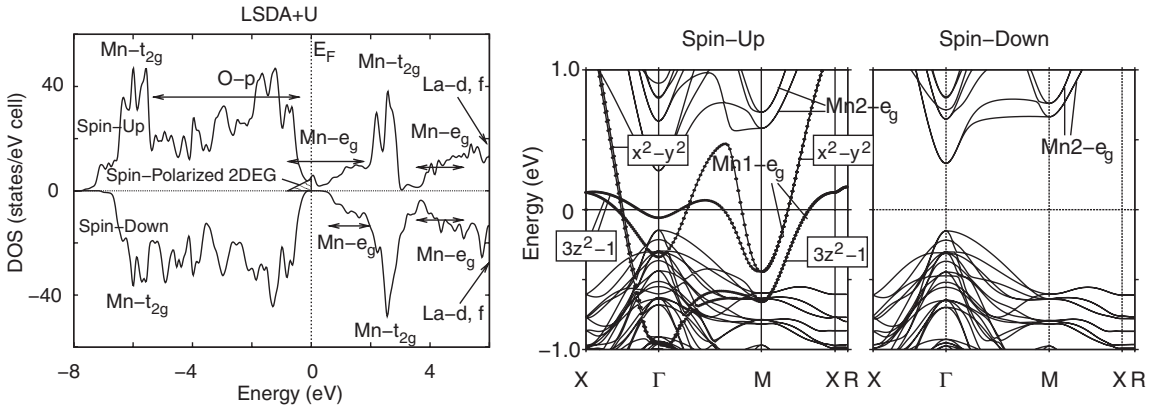

FIG. 5. Total densities of states for the $(LMO)_1/(SMO)_7$ superlattice for the majority and the minority spins (top) and the band structure in the vicinity of the Fermi energy (bottom). The symmetry points are Γ $(0, 0, 0)$, X $(1, -1, 0)$, M $(0, 2, 0)$, and R $(1, -1, -2a/c)$ in units of $\pi/2a$, a being the in-plane lattice constant. The symbols Mn1 and Mn2 indicate the first and the second layer atoms, respectively, next to the interface.

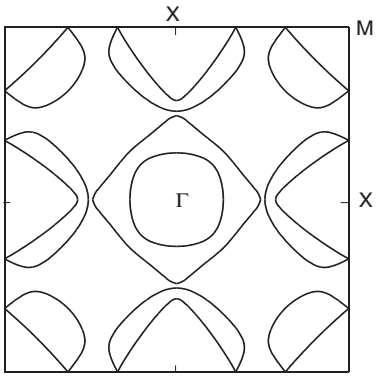

FIG. 6. The Fermi surface of $(LMO)_1/(SMO)_7$ shown in the interface Brillouin zone.

energy and outside the energy range of Fig. 5. In contrast to this, since the second layer manganese moments are antiferromagnetically organized, the Mn2-e_g states occur in both the minority- and the majority-spin channels as seen from the figure.

As discussed earlier, the partially occupied e_g states mediate a ferromagnetic double exchange between the t_{2g} core spins, which competes with the antiferromagnetic superexchange. This double exchange is directional in nature in the sense that its strength in the xy plane or along the z axis depends on the occupancy of the individual e_g orbitals ($x^2 - y^2$ and $3z^2 - 1$) [17,18]. Since we have both orbitals significantly occupied, as seen from the band plot of Fig. 5, this leads to a strong double exchange both in the first MnO_2 layers and between these layers across the interface, resulting in the layer ferromagnetic structure as shown in Fig. 1.

The interface Fermi surface, shown in Fig. 6, is constituted out of the Mn1-e_g ($x^2 - y^2$ and $3z^2 - 1$) states, and their orbital characters may be inferred from the band structure shown in Fig. 5. The Fermi surface consists of electronlike pockets at the Γ and M points and holelike pockets centered at the X points. The holes have relatively higher mass, so that the transport along the interface may be expected to be electronlike.

Although the interface suggested in this Letter has not been grown to our knowledge (but is certainly possible to grow), it is encouraging that there are several experimental works on the LMO/SMO superlattices which seem to support the existence of a ferromagnetic state at the interface [17,24,25]. It would be gratifying if the spin-polarized 2DEG can be established experimentally in these oxide systems.

In summary, our density-functional studies suggest the formation of a fully spin-polarized 2DEG at the $LaMnO_3$ layer embedded in a thick $SrMnO_3$ bulk. This occurs due to the confinement of the La electrons near the interface because of the electrostatic potential of the positively charged La layer. These electrons occupy the Mn-e_g states near the interface, mediating a Zener double exchange, which stabilizes a ferromagnetic structure of the Mn spins and the electrons become, in turn, completely spin-polarized due to the magnetic fields of the Mn atoms. The Néel G-type antiferromagnetism of the bulk $SrMnO_3$ is retained in the second MnO_2 layer from the interface and beyond. We note that earlier experiments have observed a fully spin-polarized 2DEG but with an external magnetic field present, e.g., in the modulation-doped CdMnTe quantum structures and for the lowest Landau level in the GaAs/AlGaAs quantum wells [26]. The complete spin polarization of the 2DEG without any external magnetic field promises to be a novel feature for the perovskite oxide interfaces.

We acknowledge support of this work by the U.S. Department of Energy through Grant No. DE-FG02-00ER45818.

[1] A. Ohtomo *et al.*, Nature (London) **419**, 378 (2002).
[2] Z. S. Popović and S. Satpathy, Phys. Rev. Lett. **94**, 176805 (2005).
[3] D. R. Hamann *et al.*, Phys. Rev. B **73**, 195403 (2006).
[4] S. Okamoto *et al.*, Phys. Rev. Lett. **97**, 056802 (2006).
[5] M. Hujiben *et al.*, Nature Mater. **5**, 556 (2006); A. Ohtomo and H. Y. Hwang, Nature (London) **427**, 423 (2004).
[6] D. R. Hang *et al.*, Appl. Phys. Lett. **89**, 092116 (2006).
[7] A. Tsukazaki *et al.*, Science **315**, 1388 (2007).
[8] N. Reyren *et al.*, Science **317**, 1196 (2007).
[9] P. Blaha *et al.*, WIEN2K, "An Augmented Plane Wave + Local Orbitals Program for Calculating Crystal Properties" (Karlheinz Schwarz, Technische Universitat Wien, Austria, 2001), ISBN 3-9501031-1-2.
[10] O. K. Andersen and O. Jepsen, Phys. Rev. Lett. **53**, 2571 (1984).
[11] J. P. Perdew and Y. Wang, Phys. Rev. B **45**, 13 244 (1992); J. P. Perdew *et al.*, Phys. Rev. Lett. **77**, 3865 (1996).
[12] P. Larson, Z. Popovic, and S. Satpathy, Phys. Rev. B **77**, 245122 (2008).
[13] A. J. Millis, Phys. Rev. B **55**, 6405 (1997).
[14] S. Satpathy, Z. S. Popović, and F. R. Vukajlovic, Phys. Rev. Lett. **76**, 960 (1996).
[15] D. Feinberg *et al.*, Phys. Rev. B **57**, R5583 (1998).
[16] P. W. Andersen and H. Hasegawa, Phys. Rev. **100**, 675 (1955); C. Zener, Phys. Rev. **82**, 403 (1951); P.-G. de Gennes, Phys. Rev. **118**, 141 (1960).
[17] H. Yamada *et al.*, Appl. Phys. Lett. **89**, 052506 (2006).
[18] B. R. K. Nanda and S. Satpathy, Phys. Rev. B **78**, 054427 (2008).
[19] W. R. L. Lambrecht *et al.*, Phys. Rev. B **41**, 2813 (1990).
[20] W. E. Pickett and D. J. Singh, Phys. Rev. B **53**, 1146 (1996).
[21] H. Meskine, H. König, and S. Satpathy, Phys. Rev. B **64**, 094433 (2001).
[22] S. K. Mishra *et al.*, Phys. Rev. B **55**, 2725 (1997).
[23] Z. Zhang and S. Satpathy, Phys. Rev. B **44**, 13 319 (1991).
[24] S. J. May *et al.*, Phys. Rev. B **77**, 174409 (2008).
[25] Ş. Smadici *et al.*, Phys. Rev. Lett. **99**, 196404 (2007).
[26] A. Lemaitre *et al.*, Phys. Rev. B **62**, 5059 (2000); S. Melinte *et al.*, Phys. Rev. Lett. **84**, 354 (2000).